

Article

Fingerprint-Based Machine Learning Approach to Identify Potent and Selective 5-HT_{2B}R Ligands

Krzysztof Rataj ^{1,*} , Adam Andor Kelemen ², José Brea ³, María Isabel Loza ³, Andrzej J. Bojarski ^{1,*}  and György Miklós Keserü ^{2,*} 

¹ Department of Medicinal Chemistry, Institute of Pharmacology, Polish Academy of Sciences, 12 Smętna Street, 31-343 Krakow, Poland; krzysiek.firmowy.pan@gmail.com

² Medicinal Chemistry Research Group, Research Centre for Natural Sciences, Hungarian Academy of Sciences, Magyar tudósok krt. 2, H1117 Budapest, Hungary; kelemen.adam@ttk.mta.hu

³ Grupo de Investigación "BioFarma" USC, Centro de Investigación CIMUS, Planta 3ª, Avd. de Barcelona s/n, 15782 Santiago de Compostela, Spain; pepo.brea@usc.es (J.B.); mabel.loza@usc.es (M.I.L.)

* Correspondence: bojarski@if-pan.krakow.pl (A.J.B.); gy.keseru@ttk.mta.hu (G.M.K.);
Tel.: +48-12-662-3365 (A.J.B.); +36-1-382-6821 (G.M.K.)

Academic Editor: F. Javier Luque

Received: 16 April 2018; Accepted: 7 May 2018; Published: 10 May 2018



Abstract: The identification of subtype-selective GPCR (G-protein coupled receptor) ligands is a challenging task. In this study, we developed a computational protocol to find compounds with 5-HT_{2B}R versus 5-HT_{1B}R selectivity. Our approach employs the hierarchical combination of machine learning methods, docking, and multiple scoring methods. First, we applied machine learning tools to filter a large database of druglike compounds by the new Neighbouring Substructures Fingerprint (NSFP). This two-dimensional fingerprint contains information on the connectivity of the substructural features of a compound. Preselected subsets of the database were then subjected to docking calculations. The main indicators of compounds' selectivity were their different interactions with the secondary binding pockets of both target proteins, while binding modes within the orthosteric binding pocket were preserved. The combined methodology of ligand-based and structure-based methods was validated prospectively, resulting in the identification of hits with nanomolar affinity and ten-fold to ten thousand-fold selectivities.

Keywords: target selectivity; G-protein coupled receptor; 5-HT_{2B}R; chemical fingerprint

1. Introduction

There is an increasing need of efficacious CNS (central nervous system) drugs with reduced off-target activity that often connected to notable subtype selectivity. Modulated by one of the major neurotransmitters, serotonergic receptors play a central role in many neuropsychiatric indications [1]. A significant number of drugs was introduced to the market targeting different 5-HT subtypes ranging from 5-HT₁₋₇R [2]. Rational drug design of subtype selectivity remained a challenge in many cases.

The continuously growing number of available relevant class A GPCR (G-protein coupled receptor) X-ray structures (bovine rhodopsin [3,4], β_2 AR [5], 5-HT_{1B}R [6], 5-HT_{2B}R [7–9], D₃R [10], M₂R [11], etc.) revealed certain important structural motifs of molecular recognition and ligand binding, including determinants of selectivity across the certain subtypes. GPCRs consist of seven transmembrane helices (and the additional intramembrane helix 8) connected in a bunch through 3-3 intracellular, and extracellular loops. Beyond the highly conserved amino acid residues localized across the helices either in the proximity of the binding pocket, or participating in the well-established DRY [12], Np_{xx}Y [13], and P-I-F motifs [14], or in the conserved disulfide bridge [15], the most conspicuous differences are present in the extracellular vestibule near the extracellular loop 2 (ECL2)

region, which impacts subtype selectivity [16]. The role of the 5-HT_{2B} receptor has been implicated in a number of diseases including migraines [17–19], chronic heart disease [20], and irritable bowel syndrome (IBS) [21]. The chemical space of known 5-HT_{2B}R ligands might be represented by a couple of chemotypes (presented in Figure 1). Examples of high affinity 5-HT_{2B}R compounds showing selectivity against 5-HT_{1B}R are represented by triazines (1) [21], piperidines (2, 3), pyrimidines (e.g., RS-127445 (4)) [22], arylpiperazines (m-CPP [23], EGIS-7625 (5) [24]), tetrahydro-β-carbolines (LY-23728 (6), LY-272015, LY-266097) [25], and aryl ureas (SB-200646A (7), SB-204741, SB-215505) [26]. Interestingly, the contribution of in silico methods to the discovery of novel 5-HT_{2B}R ligands is rather limited [27]. Understanding the key drivers of subtype selectivity, here we report the identification of novel selective 5-HT_{2B}R ligands using a combination of ligand-based and structure-based methods.

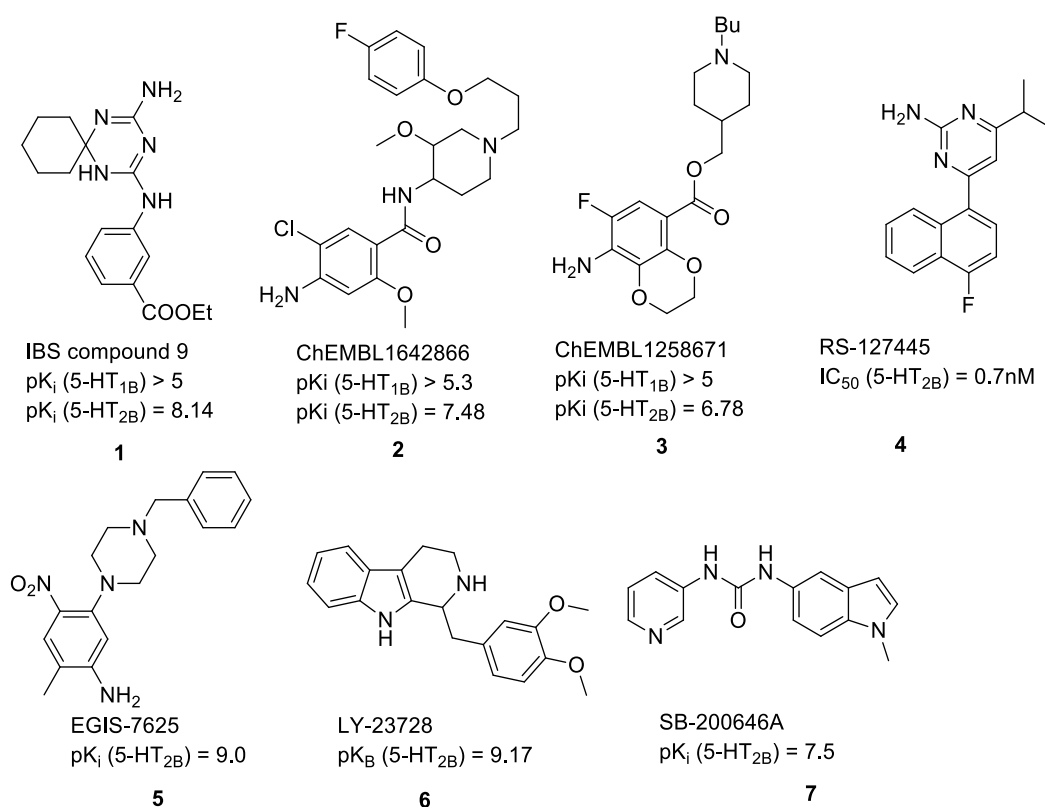


Figure 1. Representative 5-HT_{2B}R ligands (compounds 1–3 with available 5-HT_{1B}R and 5-HT_{2B}R binding affinity data, and examples of clinical candidates 4–7).

At the first stage of screening, we applied machine learning tools [28] trained on the available structural information of known h5-HT_{1B}R and h5-HT_{2B}R ligands. Started from the main principle of fragment-based drug design (FBDD), these compounds were represented by Neighbouring Substructures Fingerprint (NSFP) [29], which opens the possibilities of quickly creating fragment libraries with desired target-specific, class-specific, or even family-specific properties. This new methodology is based on connections between SMARTS (SMiles ARbitrary Target Specification) patterns for finding doublets or triplets of small substructures that constitute a larger fragment. Analyzing these structural moieties, machine learning methods [30,31] are applied to recognize non-typical, activity-specific fragments for a particular target or a group of targets. Key-based substructural fingerprints depict the occurrences of a predefined set of chemical subgroups (keys) [32] within the target molecule. However, the standard key-based representations do not provide sufficient structural information. The substructures may be arranged in various ways, resulting in a vast set of possible outcomes from a single fingerprint. This may lead to ambiguities in the process of classification of active and inactive compounds, resulting in a high false positive rate. These flaws may

be overcome by the addition of substructural connectivity data and combining this methodology with structure-based approaches.

A thorough analysis of the crystal structures of aminergic GPCR proteins revealed that most of the receptors have a secondary binding pocket (SBP) [16] that is formed at the extracellular part of the protein by the participation of the ECL2. This site contains a significant proportion of non-conserved amino acids across certain aminergic GPCRs that provides an opportunity to obtain subtype selectivity. Previously, we showed [33] that a docking strategy towards the SBP was able to identify bitopic compounds with improved affinity and selectivity. In our present study, we combined both methodologies, i.e., the fragment-based NSFP fingerprint with docking. Applying this approach for 2B and 1B serotonin receptors, we were able to identify new and selective 5-HT_{2B}R ligands, providing potential chemical starting points for further optimization.

2. Results and Discussion

2.1. Compilation of the Training Sets for Machine Learning-Based Classification

In this study, we built a NSFP fingerprint-based machine learning model using in vitro activity data available for human 5-HT_{1B}R and 5-HT_{2B}R receptors in ChEMBL (biochemical database curated by the European Molecular Biology Laboratory) [34]. The compounds were divided into actives and inactives using binding affinity thresholds. Since our design concept was based on the role of the secondary binding pocket in selectivity, only compounds with 22 or more heavy atoms were considered, as they are more likely to bind to both the orthosteric binding pocket (OBP) and SBP of 5-HT_{1B}R and 5-HT_{2B}R.

The active/inactive sets were selected based on binding affinity recalculated from various units reported in the ChEMBL to K_i (actives: K_i ≤ 500 nM, inactives: K_i ≥ 1000 nM). In this way, four sets were acquired (summarized in Table 1): active for 5-HT_{1B} (1B_{active}), active for 5-HT_{2B} (2B_{active}), inactive for 5-HT_{1B} (1B_{inactive}), and inactive for 5-HT_{2B} (2B_{inactive}). 5-HT_{1B} actives and 5-HT_{2B} inactives, and 5-HT_{2B} actives and 5-HT_{1B} inactives were used for 1B_{selective} and 2B_{selective} subsets. The nonselective subset contains compounds that are active on both 5-HT_{1B} and 5-HT_{2B} receptors.

Table 1. Active, inactive, and selective 5-HT_{1B} and 5-HT_{2B} ligands retrieved from the ChEMBL with at least 22 heavy atoms.

| Receptor | Number of Actives ¹ | Number of Inactives ² | Number of Selectives ³ |
|--------------------|--------------------------------|----------------------------------|-----------------------------------|
| 5-HT _{1B} | 858 (1011) | 339 (477) | 86 |
| 5-HT _{2B} | 478 (718) | 259 (351) | 33 |

¹ K_i ≤ 500 nM; ² K_i ≥ 1000 nM; ³ Classified as 5-HT_{2B} selective for being active at 5-HT_{2B}R, and inactive at 5-HT_{1B}R; numbers in parenthesis are the total number of all actives without size-filtering.

Altogether, seven training sets were used for building machine learning models (1–2. actives, 3–4. inactives, 5–6. selectives for both 1B and 2B receptor subtypes, and 7. nonselectives).

2.2. Building NSFP-Based Machine Learning Model

NSFP fingerprints were calculated for all of the compound sets using Klekota–Roth fingerprint (KRFP) substructure keys. A series of machine learning classifiers were created that were aimed at properly discriminating compounds. Activity classifier for 2B (2B^{activity}) was built using 2B_{active} and 2B_{inactive} compounds. Selectivity classifier (2B^{selectivity}) for 2B was built using 2B_{selective} and nonselective compounds in order to predict the putative selectivity of screened compounds. The same procedure was applied to 1B with its selective sets, resulting in 1B^{selectivity} and 2B^{selectivity} classifiers. Altogether, we developed two activity (for 5-HT_{1B}R and 5-HT_{2B}R) and two selectivity (for 5-HT_{1B}R and 5-HT_{2B}R) classifiers using known active, inactive, selective, and non-selective 5-HT_{1B}R and 5-HT_{2B}R ligands. Final models were selected from the total of 4 × 117 classifiers based on the highest acquired

Matthews correlation coefficient (MCC) values. These models were used for filtering the in-stock MCule database. The summary of the model development is shown in Figure 2.

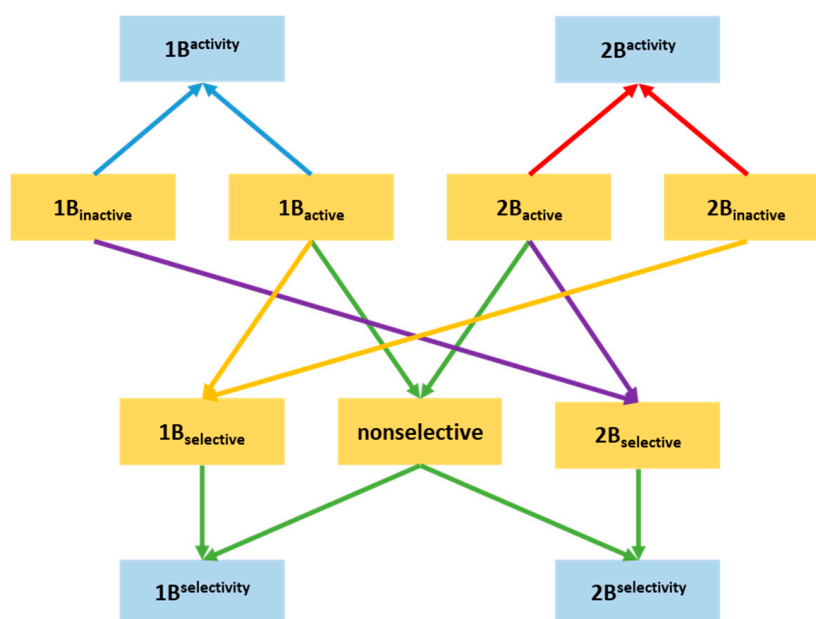


Figure 2. Depiction of Neighbouring Substructures Fingerprint (NSFP) representations of constructed compound sets (orange) and machine learning models (blue).

2.3. Prospective Machine Learning-Based Classification

First, NSFP fingerprints have also been calculated for the entire MCule database [35] of commercially available compounds. Next, each compound was classified using the four machine learning models. If a compound's classification by $2B^{\text{activity}}$ was positive (compound classified as 2B active) and classification by $1B^{\text{activity}}$ was negative (compound classified as 1B inactive), the compound was treated as a putative 2B selective compound (${}^12B_{\text{selective}}$). If the opposite was true (compound classified as 1B active and 2B inactive), the compound was regarded as a putative 1B selective compound (${}^11B_{\text{selective}}$). Compounds achieving any other combination of classification results were disregarded from further research.

The second round of classification consisted of validating the compounds against the $1B^{\text{selectivity}}$ and $2B^{\text{selectivity}}$ selectivity classifiers. If a ${}^12B_{\text{selective}}$ compound was classified as positive by the $2B^{\text{selectivity}}$ and negative by the $1B^{\text{selectivity}}$, the compound was regarded as ${}^22B_{\text{selective}}$. In any other case, the compound was discarded. The summary of the prospective classification is presented in Figure 3.

The in-stock MCule database containing 4.8 M molecules was filtered prospectively in an activity-classification and consecutively in a selectivity-classification step resulting in 24,849 putative 5-HT_{2B} selective compounds (Figure 4).

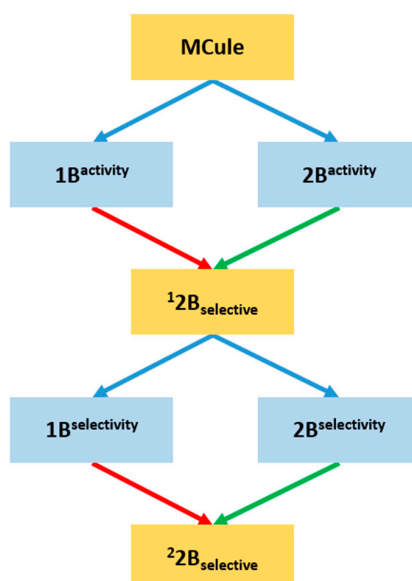


Figure 3. Classification procedure for putative 2B selective compounds. Green arrows represent positive classification and red arrows represent negative classification.

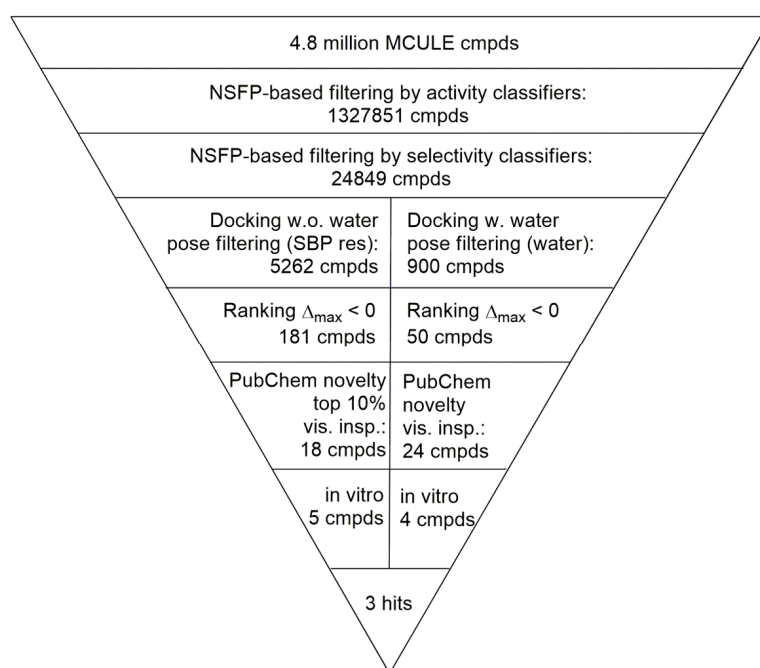


Figure 4. Flowchart of the virtual screening cascade used for the identification of 5-HT_{2B} selective hits.

2.4. Virtual Screening of the Prefiltered Set Classified by Machine Learning

In the next sequential filtering step, the pre-filtered 5-HT_{2B} selective compound set of 24,849 compounds was subjected to two complementary docking workflows (i) considering non-conserved amino acid pairs and ranking-based consensus scoring; and (ii) accounting for water molecules (Figure 4). The set of 24,849 putative 5-HT_{2B} selective compounds was docked into four crystal structures available to date (PDB (Protein Data Bank) ID: 4IAQ, 4IAR [6] for h5-HT_{1B}R, and 4IB4 [7], 4NC3 [8] for h5-HT_{2B}R). Our docking constraints involved forming a hydrogen bond to Asp^{3.32} (Ballesteros–Weinstein numbering in superscript) [36] that anchors the charged amines of aminergic ligands [37] and any interactions with the designated non-conserved amino acid pairs

present in the SBPs of the two receptors based on the work of Michino et al. [38] (see Figure 5A,B). Each pose-filtered ligand was ranked at the four receptors based on their Glide scores. The consensus scoring [39] resulted in the selection of 181 compounds showing preference to 5-HT_{2B}R based on their rankings. The set of 181 ligands was sorted by their Δ_{\max} values = [(RANK at 4IB4 receptor) + (RANK at 4NC3 receptor)] - [(RANK at 4IAQ receptor) + (RANK at 4IAR receptor)]. The top 10% (18 ligands) were subjected to a novelty check against PubChem, and were selected for visual inspection, analyzing their binding modes. This nominated five compounds (**8**, **10**, **11**, **12**, and **13** marked with “a” in Table 2) with the largest difference of ranks obtained on 5-HT_{2B} and 5-HT_{1B} structures for in vitro tests.

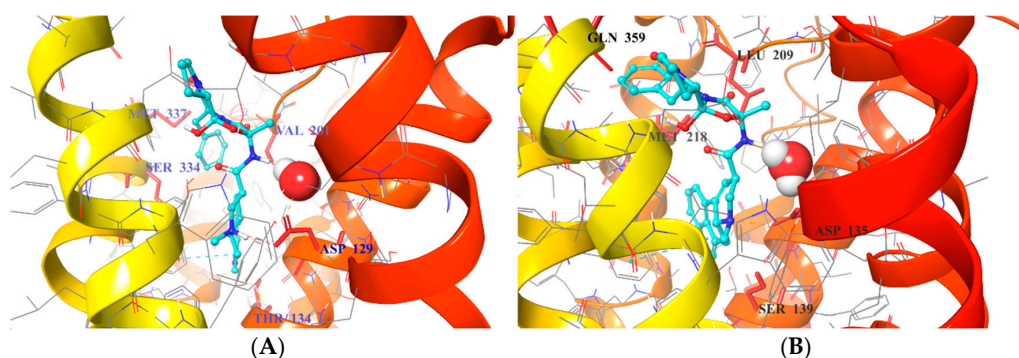


Figure 5. Residues (red) used in pose filtering for 5-HT_{1B}R (PDB ID: 4IAQ) panel (A) and 5-HT_{2B}R X-ray structures (PDB ID: 4IB4) panel (B); Water molecules forming interactions with the Asp^{3.32} shown as a sphere representation.

Table 2. Structures and measured in vitro assay data of top-ranked compounds (sorted by percentage of inhibition and K_i (nM) in h5-HT_{2B}R competition binding assay). Values represent the mean ± SD of three independent assays with duplicate measurements.

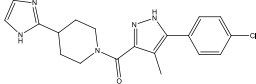
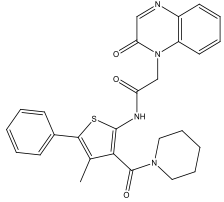
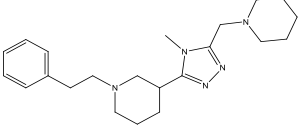
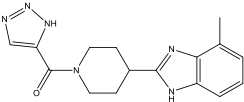
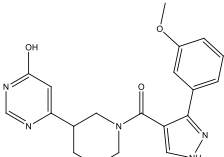
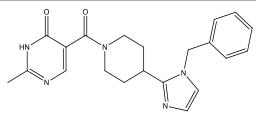
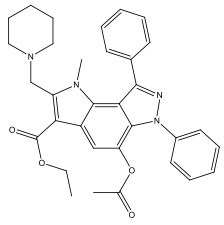
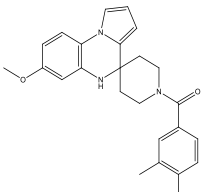
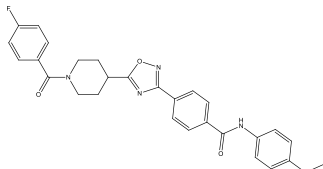
| Compound | ID | 5-HT _{1B} (%) ¹ | 5-HT _{2B} (%) ¹ | 5-HT _{1B} (nM) ² | 5-HT _{2B} (nM) ² |
|---|-----------------------|-------------------------------------|-------------------------------------|--------------------------------------|--------------------------------------|
|  | 8^a | - | - | 2934.7 ± 321.3 | 0.3 ± 0.07 |
|  | 9^b | - | - | 2099 ± 622.2 | 235.1 ± 15.9 |
|  | 10^a | 7 ± 4 | - | - | 2612.9 ± 422.1 |
|  | 11^a | 12 ± 4 | 40 ± 3 | - | - |
|  | 12^a | 7 ± 1 | 36 ± 4 | - | - |

Table 2. Cont.

| Compound | ID | 5-HT _{1B} (%) ¹ | 5-HT _{2B} (%) ¹ | 5-HT _{1B} (nM) ² | 5-HT _{2B} (nM) ² |
|--|-----------------|-------------------------------------|-------------------------------------|--------------------------------------|--------------------------------------|
|  | 13 ^a | 19 ± 3 | 34 ± 4 | - | - |
|  | 14 ^b | 26 ± 4 | 34 ± 4 | - | - |
|  | 15 ^b | 28 ± 3 | 31 ± 4 | - | - |
|  | 16 ^b | 1 ± 1 | 24 ± 4 | - | - |

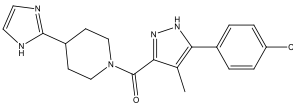
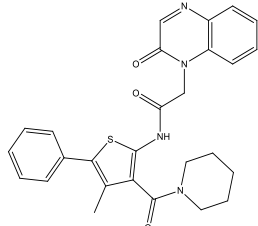
¹ Percentage of inhibition measured at 10 μM concentration; ² K_i measured (reported in nM units) if percentage of inhibition exceeded 50%; ^a Selection not accounting waters, ^b Selection accounting waters.

As a complementary approach, we have filtered a second pool of compounds, considering the structural waters found in the X-ray structures of the receptors (PDB ID: 4IAQ [6] for h5-HT_{1B}R, and 4IB4 [7] for h5-HT_{2B}R). In both structures, one water molecule anchoring the oxo group of the ergoline ligands' amide moiety with the Asp^{3.32} in TM3 was considered. Whereas the waters settle the actual position and conformation of the co-crystallized ligand, they might also govern other ligands to reach the SBP (see Figure 5). Interactions to these water molecules or directly to the protein were used for pose filtering, yielding 900 ligands with satisfactory binding modes. The 900 pose-filtered compounds were ranked, and $\Delta_{\max} = (\text{RANK at 4IB4 receptor}) - (\text{RANK at 4IAQ receptor})$ values were calculated. The ligands were sorted by Δ_{\max} values, and 50 structurally diverse compounds with high rank differences (i.e., $\Delta_{\max} \ll 0$) were selected for novelty screening. We identified 24 compounds with no known similar and active analogues in PubChem [40] that were subjected to visual inspection selecting four hits (9, 14, 15, and 16 marked with "b" in Table 2) with feasible binding mode (compounds marked with "b" in Table 2).

Altogether nine compounds that were predicted to be 2B selective were selected for competition binding assay for 5-HT_{1B}R and 5-HT_{2B}R (Table 2). Three hit compounds were identified (compounds 8–10), showing preference towards the desired 5-HT_{2B}R target over the 5-HT_{1B}R off-target. Moreover, selectivity of two hit 5-HT_{2B}R ligands 8 and 9 over four serotonin receptors (5-HT_{1A}, 5-HT_{2A}, 5-HT₆, and 5-HT₇) was confirmed (Table 3).

Our sequential screening protocol was able to identify potent and selective compounds with a 33% hit rate, including a highly active (subnanomolar activity) compound with almost 10⁴ selectivity factor. The 5-HT_{2B} versus 5-HT_{1B} selectivity of the closest literature analogue (compound 17 shown in Figure 6) was not confirmed by Moss et al. [41]. Lacking the relevant 5-HT_{1B} affinity, 17 was not part of the ChEMBL training set that underlines the efficiency of the NSFP-based classification models.

Table 3. 5-HT panel screening of the best hits. Values represent the mean \pm SD of three independent assays with duplicate measurements.

| Compound | ID | 5-HT _{1A} K _i (μ M) | 5-HT _{2A} K _i (μ M) | 5-HT ₆ K _i (μ M) | 5-HT ₇ K _i (μ M) |
|---|----|--|--|---|---|
|  | 8 | >20 | >20 | 13.2 \pm 1.5 | >20 |
|  | 9 | >20 | >20 | 7.5 \pm 0.9 | >20 |

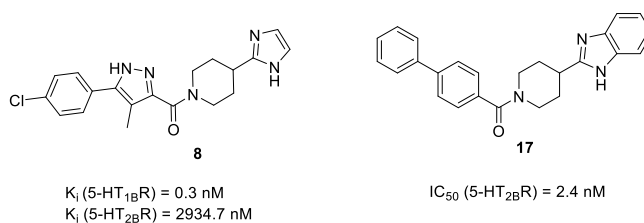


Figure 6. Structure of hit compound (8) and its closest literature analogue (17).

2.5. Binding Mode of Compound 8

The SBP of 5-HT_{2B}R, which was originally occupied by the peptide portion of the ergoline ligand, is defined by several residues of ECL2, TM5, TM7, and TM6. The 4-chlorophenyl tail of 8 occupies the same orthosteric hydrophobic cavity formed by Phe340^{6.51}, Phe341^{6.52}, Ile143^{3.40}, Trp337^{6.48}, and is stacked by π - π interactions similarly to the indole ring of ergotamine (Figure 7).

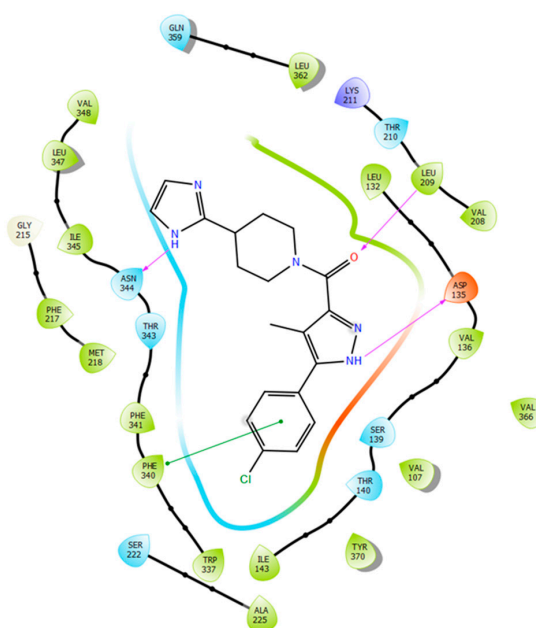


Figure 7. Two-dimensional (2D) interaction diagram of MCULE-7016689532 (8) in the 5-HT_{2B}R.

Additionally, the imidazolyl–piperidine part of the ligand is supposed to reach toward the SBP, and form a hydrogen–bond interaction with the backbone oxo group (Val208) of the same hydrophobic cleft at ECL2, such as the peptide region of ergotamine (see Figure 8). Residues Asn344^{6,55} and Met218^{5,39} are narrowing the upper chamber of the 5-HT_{2B}R binding pocket, compared with 5-HT_{1B}R. It has been shown [21] that disturbance of the water-network around the Asn344^{6,55} is the consequence of ligand binding to this chamber. Interestingly, the imidazole NH of the ligand formed a polar–polar interaction with this residue.

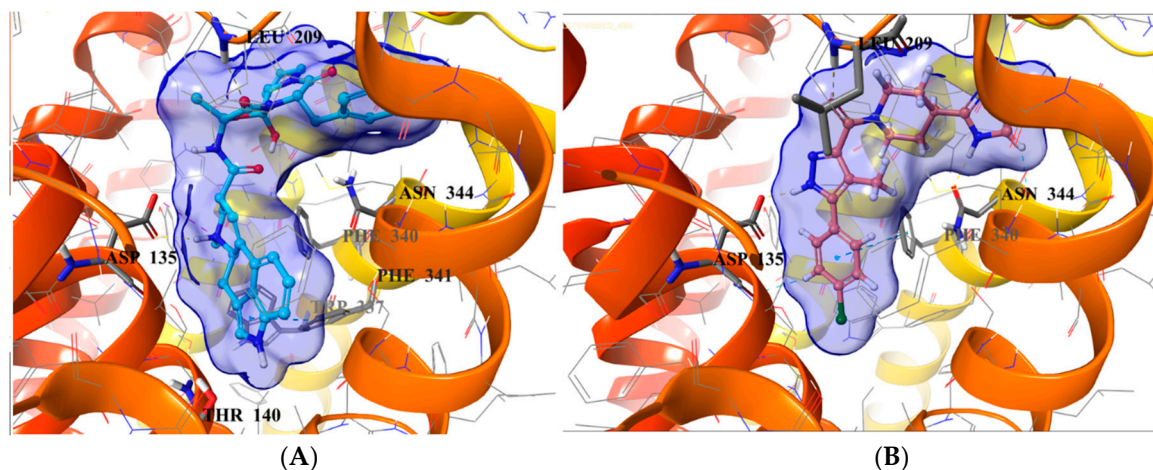


Figure 8. Binding site surfaces (blue spheres) of ergotamine panel (A) and 8 panel (B) in the 5-HT_{2B}R crystal structure. Important ligand-contacting residues are shown in thick tube representation.

3. Conclusions

In this study, we aimed identifying selective 5-HT_{2B}R ligands by virtual screening. Given the sequential and structural similarities of serotonergic receptors, we hypothesized that receptor selectivity is basically driven from the SBP. Consequently, we developed a screening strategy combining both ligand-based and structure-based approaches. For the first level of our hierarchical approach, we used NSFP and developed machine learning tools to select potential 5-HT_{2B}R selective molecules from a large database of druglike compounds. Next, this subset was subjected to docking calculations, and we identified compounds showing different interactions with the secondary binding pockets of 5-HT_{2B}R and 5-HT_{1B}R. Careful analysis of the binding mode allowed us to select nine compounds for biological testing. Out of these, three compounds showed significant 5-HT_{2B}R affinity, one in the low micromolar (10), one in the submicromolar (9), and one in the subnanomolar range (8). Compounds with submicromolar 5-HT_{2B}R affinity were further profiled against a set of serotonin receptors including 5-HT_{1A}R, 5-HT_{2A}R, 5-HT₆R, and 5-HT₇R. The best compound (8) showed $K_i = 0.3$ nM affinity and ten thousand-fold selectivity for 5-HT_{2B}R, which nominates it for in vivo testing.

4. Materials and Methods

4.1. Procedures of Machine Learning-Based Classification Model Building

Basing on the KR-NSFP representations of compounds sets, four discrimination models were built using machine learning methods: 1B^{activity} (based on 1B_{active} and 1B_{inactive} sets), 2B^{activity} (using 2B_{active} and 2B_{inactive} sets), 1B^{selectivity} (using 1B_{selective} and nonselective sets), and 2B^{selectivity} (using 2B_{selective} and nonselective sets). For each case, a series of initial models was created, using various machine learning techniques including Support Vector Machines with Radial Basis Factor and Tanimoto kernels, Naïve Bayes and Extreme Entropy Machines with Tanimoto and Sorensen kernels [30,31]. Additionally, for each method–kernel pair, a set of hyperparameters was tested, resulting in 117 initial models acquired for each final classification model. The classifiers were tested using five-fold cross-validation

methodology, and for each of the compound sets, the model with the highest MCC value (see Table 4) was selected for final classification study. The entire machine learning methodology was implemented in Python programming language using scikit-learn libraries.

The equation of the MCC values calculated for the ChEMBL training set is:

$$\text{MCC}(\text{TP}, \text{TN}, \text{FP}, \text{FN}) = \frac{\text{TP} \times \text{TN} - \text{FP} \times \text{FN}}{\sqrt{(\text{TP} + \text{FP})(\text{TP} + \text{FN})(\text{TN} + \text{FP})(\text{TN} + \text{FN})}}$$

where TP—True Positive, FP—False Positive, TN—True Negative, and FN—False Negative.

Table 4. Performance data of the activity and selectivity filters obtained on ChEMBL training set.

| Receptor | MCC of Activity Classifiers | MCC of Selectivity Classifiers |
|--------------------|-----------------------------|--------------------------------|
| 5-HT _{1B} | 0.7867 | 0.8057 |
| 5-HT _{2B} | 0.7376 | 0.8238 |

4.2. Docking-Based Evaluation of NSFP-Classified MCule Sets

4.2.1. Preparation of Ligand Sets, and Receptor Structures for Docking

Compounds used for selective ligand discovery were minimized using Schrödinger's LigPrep algorithm [42], with the pH set to 7.4 and the number of stereoisomers set to 1. For this study, crystal structures of 5-HT_{1B}R and 5-HT_{2B}R were extracted from the PDB database [43] (PDB ID: 4IAQ and 4IAR [6] for 1B, and 4IB4 [7] and 4NC3 [8] for 2B). Proteins were prepared using PrepWiz software (version 2017-4) from Schrödinger [44] and transformed into a receptor grid using Schrödinger software package [45], with the binding pocket center set to the Asp^{3.32} residue. All of the docking procedures have been conducted using Schrödinger's Glide software [46], with precision set to standard precision (SP) and varying the number of reported docking poses (5 or 10).

4.2.2. Evaluation of the Docking Results

The ²B_{selective} set was docked to the crystal structures of both 5-HT_{1B} and 5-HT_{2B} receptors (PDB ID: 4IAQ, 4IAR for 5-HT_{1B}R and 4IB4, 4NC3 for 5-HT_{2B}R, respectively), and the number of reported poses was set to 10. Additionally, poses were filtered for interactions with the SBP characteristic amino acids (see Table 5).

Table 5. All of the interactions considered during the pose filtering phase. The blue cells represent hydrogen bonds, and the red cells represent distance criterion (≤ 5.0 Å between the compound and any atom of a residue). OBP: orthosteric binding pocket; SBP: secondary binding pocket.

| Interactions | 1B Crystals | 2B Crystals |
|--------------|-------------------------|-------------------------|
| OBP | D129 ^{3.32} | D135 ^{3.32} |
| | T134 ^{3.37} | S139 ^{3.36} |
| | S212 ^{5.42} | |
| SBP | | Q359 ^{7.32} |
| | M337 ^{6.58} | M218 ^{5.39} |
| | V201 ^{ECL2.52} | L209 ^{ECL2.52} |

Scoring of reported poses was performed using custom scoring function [39], taking into consideration the rankings of compounds based on the assigned Glide docking score. It compares the numerical sum of the ranks of all of the poses acquired by a compound in both crystals of the target protein with those found in both crystals of the antitarget:

$$\Delta_{\text{max}} = [\sum(\text{rank}_{\text{target}}) - \sum(\text{rank}_{\text{antitarget}})]$$

Since better rankings have lower numerical values (a pose with rank 1 is better than a pose with rank 5), if the compound's $\Delta_{\max} < 0$, it was considered target-selective. For further research, the compounds with the lowest Δ_{\max} were considered, as the difference in ranks between target and antitarget were the highest. Finally, the docking binding modes of the top 10% (18 ligands) were visually inspected, and five compounds (**8**, **10**, **11**, **12**, and **13** marked with "a" in Table 2) were hand-picked for in vitro validation.

The second approach included screening for interactions with water molecules buried within the binding pockets of target receptors. Of all four crystal structures of the receptors, only two contained water within the three-dimensional (3D) model: 4IAQ (1B) [6] and 4IB4 (2B) [7]. Therefore, these two structures were used in a second docking study conducted with constraints set for either a hydrogen bond/salt bridge to Asp^{3.32}, or a hydrogen bond with water 2020 (4IAQ) or 2004 (4IB4). Docked compounds were filtered for proper interactions with the water molecule/Asp^{3.32} residue, and their specificity. The binding mode of the filtered compounds was checked manually, and they were subjected to a novelty check by PubChem [40] before testing with the NSFP.

The 900 pose-filtered docked ligands were first clustered by structural similarity, and a diverse set of 50 cluster centroids were subjected to novelty check using the PubChem engine. Compounds having no similar compounds or no tested analogues, or having tested but inactive analogues, were prioritized. This process yielded 24 ligands in total, out of which four compounds were selected (**9**, **14**, **15**, and **16**, marked with "b" in Table 2) after visual inspection for in vitro testing.

4.3. Procedures of In Vitro Screening Assays

All of the tested compounds were purchased via MCule, Inc. (Palo Alto, CA, USA). The compounds were tested for their ability to displace radioligand from the membrane of 5-HT_{1B}R and 5-HT_{2B}R-expressing cells. The first test was performed with a 10- μ M concentration of a compound, and the inhibition percentage was calculated. If the value was above 50%, a full affinity screening was performed, and the data was gathered as K_i with units reported as nM.

4.3.1. Competition Binding in Human 5-HT_{1B} Receptor

Serotonin 5-HT_{1B}R competition binding experiments were carried out in a polypropylene 96-well plate. In each well, 5 μ g of membranes from a HeLa-5-HT_{1B} cell line that was prepared in our laboratory (Lot: A001/14-11-2011, protein concentration = 3179 μ g/mL), 1.5 nM [³H]-GR125743 (83.9 Ci/mmol, 0.1 mCi/mL, Perkin Elmer NET1172100UC, K_D = 0.74 nM), the studied compounds and the reference compound were incubated. Non-specific binding was determined in the presence of GR55562 10 μ M (TOCRIS 1054), and total binding was determined in the absence of any unlabeled compound. The reaction mixture (Vt: 250 μ L/well) was incubated at 25 °C for 90 min. Then, 200 μ L was transferred to a GF/C 96-well plate (Millipore, Madrid, Spain) pretreated with 0.5% of PEI and treated with binding buffer (Tris-HCl 50 mM, EDTA 1 mM, MgCl₂ 10 mM, pH = 7.4). Afterwards, it was filtered and washed four times with 250 μ L of wash buffer (Tris-HCl 50 mM, pH = 7.4), before measuring in a microplate beta scintillation counter (Microbeta Trilux, PerkinElmer, Madrid, Spain). 5-carboxytryptamine was included as a reference compound in all of the assays. Compounds were first tested at 10 micromolar; those compounds showing a percentage of displacement of specific binding higher than 50% were classified as active compounds, and K_i values were determined by means of concentration-response curves.

4.3.2. Competition Binding in Human 5-HT_{2B} Receptor

Serotonin 5-HT_{2B}R competition binding experiments were carried out in a polypropylene 96-well plate. In each well, 5 μ g of membranes from a CHO-5-HT_{2B} cell line prepared in our laboratory (Lot: A003/27-03-2012, protein concentration = 3431 μ g/mL), 1 nM [³H]-LSD (82.4 Ci/mmol, 1 mCi/mL, PerkinElmer NET638250UC, K_D = 0.57 nM), the studied compounds and the reference compound were incubated. Non-specific binding was determined in the presence of 5-HT 50 μ M

(Sigma H9523), and total binding was determined in the absence of any unlabeled compound. The reaction mixture (Vt: 250 μ L/well) was incubated at 37 °C for 30 min. Then, 200 μ L was transferred to a GF/C 96-well plate (Millipore, Madrid, Spain) pretreated with 0.5% of PEI and treated with binding buffer (Tris-HCl 50 mM, Ascorbic acid 0.1%, CaCl₂ 4 mM, pH = 7.4). Afterwards, it was filtered and washed four times with 250 μ L of wash buffer (Tris-HCl 50 mM, pH = 7.4) before measuring in a microplate beta scintillation counter (Microbeta Trilux, PerkinElmer, Madrid, Spain). Methysergide was included as a reference compound in all of the assays. Compounds were first tested at 10 micromolar, and those compounds showing a percentage of displacement of specific binding higher than 50% were classified as active compounds, and K_i values were determined by means of concentration-response curves.

4.3.3. Competition Binding in Human 5-HT_{1A}, 5-HT_{2A}, 5-HT₆ and 5-HT₇ Receptors

HEK293 cells with stable expression of human serotonin 5-HT_{1A}R, 5-HT_{2A}R, 5-HT₆R, or 5-HT_{7b}R receptor (all prepared with the use of Lipofectamine 2000) were maintained at 37 °C in a humidified atmosphere with 5% CO₂, and were grown in Dulbecco's Modified Eagle Medium containing 10% dialyzed fetal bovine serum and 500 mg/mL G418 sulfate. For the preparation of membranes, cells were subcultured in 10-cm diameter dishes, grown to 90% confluence, washed twice with prewarmed to 37 °C phosphate-buffered saline (PBS), and were pelleted by centrifugation (200 g) in PBS containing 0.1 mM of EDTA and 1 mM of dithiothreitol. Prior to membrane preparations, pellets were stored at −80 °C.

Cell pellets were thawed and homogenized in 20 volumes of assay buffer using an Ultra Turrax tissue homogenizer and centrifuged twice at 35,000 g for 20 min at 4 °C, with incubation for 15 min at 37 °C in between. The composition of the assay buffers was as follows: for 5-HT_{1A}R: 50 mM Tris-HCl, 0.1 mM EDTA, 4 mM MgCl₂, 10 μ M pargyline, and 0.1% ascorbate; for 5-HT_{2A}R: 50 mM Tris-HCl, 0.1 mM EDTA, 4 mM MgCl₂, and 0.1% ascorbate; for 5-HT₆R: 50 mM Tris-HCl, 0.5 mM EDTA, and 4 mM MgCl₂, for 5-HT_{7b}R: 50 mM Tris-HCl, 4 mM MgCl₂, 10 μ M pargyline, and 0.1% ascorbate. All of the assays were incubated in a total volume of 200 μ L in 96-well microtiter plates for 1 h at 37 °C, except for 5-HT_{1A}R and 5-HT_{2A}R, which were incubated at room temperature for 1 h and 1.5 h, respectively. The process of equilibration was terminated by rapid filtration through Unifilter plates with a 96-well cell harvester, and the radioactivity retained on the filters was quantified on a Microbeta plate reader (PerkinElmer, Waltham, MA, USA).

For displacement studies, the assay samples contained as radioligands: 1.5 nM of [³H]-8-OH-DPAT (135.2 Ci/mmol, K_D = 1.5 nM) for 5-HT_{1A}R; 2 nM of [³H]-Ketanserin (53.4 Ci/mmol, K_D = 2 nM) for 5-HT_{2A}R; 2 nM of [³H]-LSD (83.6 Ci/mmol, K_D = 2 nM) for 5-HT₆R, or 0.6 nM of [³H]-5-CT (39.2 Ci/mmol, K_D = 0.6 nM) for 5-HT_{7R}. Non-specific binding is defined with 10 μ M of 5-HT in 5-HT_{1A}R and 5-HT_{7R} binding experiments, whereas 10 μ M of chlorpromazine or 10 μ M of methiothepin were used in 5-HT_{2A}R and 5-HT₆R assays, respectively. Each compound was tested in triplicate at seven concentrations (10^{−10}–10^{−4} M). Reference compounds for 5-HT_{1A}R: buspirone K_i = 32.2 nM \pm 2.9; for 5-HT_{2A}R: olanzapine K_i = 5.6 nM \pm 1.1; for 5-HT₆R: olanzapine K_i = 8.8 nM \pm 1.3; and for 5-HT_{7R}: 5-CT K_i = 0.8 nM \pm 0.2. The inhibition constants (K_i) were calculated from the Cheng-Prusoff equation [47]. Results were expressed as means of at least two separate experiments.

Author Contributions: G.M.K. and A.J.B. conceived the story; K.R. performed and evaluated the fingerprint-based machine learning model; Á.A.K. performed and evaluated the docking experiments; J.B., M.I.L. and S.P. performed the in vitro assay measurements.

Funding: Á.A.K. and G.M.K. were supported by the National Brain Research Program (2017-1.2.1-NKP-2017-00002). K.R. is grateful for the ETIUDA scholarship of the National Science Center, Poland. J.B. and M.I.L. are grateful for the support from the Spanish Ministerio de Economía y Competitividad (SAF2017-85225-C3-1-R).

Acknowledgments: Authors are grateful to Grzegorz Satała for testing compounds affinity for the extended panel of serotonin receptors.

Conflicts of Interest: The authors declare no conflict of interest.

References

1. McCorvy, J.D.; Roth, B.L. Structure and function of serotonin G protein-coupled receptors. *Pharmacol. Ther.* **2015**, *150*, 129–142. [[CrossRef](#)] [[PubMed](#)]
2. Kitson, S.L. 5-hydroxytryptamine (5-HT) receptor ligands. *Curr. Pharm. Des.* **2007**, *13*, 2621–2637. [[CrossRef](#)] [[PubMed](#)]
3. Costanzi, S.; Siegel, J.; Tikhonova, I.; Jacobson, K. Rhodopsin and the Others: A Historical Perspective on Structural Studies of G Protein-Coupled Receptors. *Curr. Pharm. Des.* **2009**, *15*, 3994–4002. [[CrossRef](#)] [[PubMed](#)]
4. Palczewski, K.; Kumasaka, T.; Hori, T.; Behnke, C.A.; Motoshima, H.; Fox, B.A.; Le Trong, I.; Teller, D.C.; Okada, T.; Stenkamp, R.E.; et al. Crystal structure of rhodopsin: A G protein-coupled receptor. *Science* **2000**, *289*, 739–745. [[CrossRef](#)] [[PubMed](#)]
5. Cherezov, V.; Rosenbaum, D.M.; Hanson, M.A.; Rasmussen, S.G.F.; Foon, S.T.; Kobilka, T.S.; Choi, H.J.; Kuhn, P.; Weis, W.I.; Kobilka, B.K.; et al. High-resolution crystal structure of an engineered human β_2 -adrenergic G protein-coupled receptor. *Science* **2007**, *318*, 1258–1265. [[CrossRef](#)] [[PubMed](#)]
6. Wang, C.; Jiang, Y.; Ma, J.; Wu, H.; Wacker, D.; Katritch, V.; Han, G.W.; Liu, W.; Huang, X.-P.; Vardy, E.; et al. Structural basis for molecular recognition at serotonin receptors. *Science* **2013**, *340*, 610–614. [[CrossRef](#)] [[PubMed](#)]
7. Wacker, D.; Wang, C.; Katritch, V.; Han, G.W.; Huang, X.-P.; Vardy, E.; McCorvy, J.D.; Jiang, Y.; Chu, M.; Siu, F.Y.; et al. Structural Features for Functional Selectivity at Serotonin Receptors. *Science* **2013**, *340*, 615–619. [[CrossRef](#)] [[PubMed](#)]
8. Liu, W.; Wacker, D.; Gati, C.; Han, G.W.; James, D.; Wang, D.; Nelson, G.; Weierstall, U.; Katritch, V.; Barty, A.; et al. Serial Femtosecond Crystallography of G Protein-Coupled Receptors. *Science* **2013**, *342*, 1521–1524. [[CrossRef](#)] [[PubMed](#)]
9. Wacker, D.; Wang, S.; McCorvy, J.D.; Betz, R.M.; Venkatakrishnan, A.J.; Levit, A.; Lansu, K.; Schools, Z.L.; Che, T.; Nichols, D.E.; et al. Crystal Structure of an LSD-Bound Human Serotonin Receptor. *Cell* **2017**, *168*, 377–389. [[CrossRef](#)] [[PubMed](#)]
10. Chien, E.Y.T.; Liu, W.; Zhao, Q.; Katritch, V.; Han, G.W.; Hanson, M.A.; Shi, L.; Newman, A.H.; Javitch, J.A.; Cherezov, V.; et al. Structure of the human dopamine D3 receptor in complex with a D2/D3 selective antagonist. *Science* **2010**, *330*, 1091–1095. [[CrossRef](#)] [[PubMed](#)]
11. Kruse, A.C.; Hu, J.; Pan, A.C.; Arlow, D.H.; Rosenbaum, D.M.; Rosemond, E.; Green, H.F.; Liu, T.; Chae, P.S.; Dror, R.O.; et al. Structure and dynamics of the M3 muscarinic acetylcholine receptor. *Nature* **2012**, *482*, 552–556. [[CrossRef](#)] [[PubMed](#)]
12. Rovati, G.E.; Capra, V.; Neubig, R.R.; Smit, M.J.; Roovers, E.; Cotecchia, S.; Leurs, R. The highly conserved DRY motif of class A G protein-coupled receptors: Beyond the ground state. *Mol. Pharmacol.* **2007**, *71*, 959–964. [[CrossRef](#)] [[PubMed](#)]
13. Nygaard, R.; Zou, Y.; Dror, R.O.; Mildorf, T.J.; Arlow, D.H.; Manglik, A.; Pan, A.C.; Liu, C.W.; Fung, J.J.; Bokoch, M.P.; et al. The dynamic process of β_2 -adrenergic receptor activation. *Cell* **2013**, *152*, 532–542. [[CrossRef](#)] [[PubMed](#)]
14. Dror, R.O.; Pan, A.C.; Arlow, D.H.; Borhani, D.W.; Maragakis, P.; Shan, Y.; Xu, H.; Shaw, D.E. Pathway and mechanism of drug binding to G-protein-coupled receptors. *Proc. Natl. Acad. Sci. USA* **2011**, *108*, 13118–13123. [[CrossRef](#)] [[PubMed](#)]
15. Rasmussen, S.G.F.; Choi, H.-J.; Rosenbaum, D.M.; Kobilka, T.S.; Thian, F.S.; Edwards, P.C.; Burghammer, M.; Ratnala, V.R.P.; Sanishvili, R.; Fischetti, R.F.; et al. Crystal structure of the human β_2 adrenergic G-protein-coupled receptor. *Nature* **2007**, *450*, 383–387. [[CrossRef](#)] [[PubMed](#)]
16. Michino, M.; Beuming, T.; Donthamsetti, P.; Newman, A.H.; Javitch, J.A.; Shi, L. What Can Crystal Structures of Aminergic Receptors Tell Us about Designing Subtype-Selective Ligands? *Pharmacol. Rev.* **2014**, *67*, 198–213. [[CrossRef](#)] [[PubMed](#)]
17. Johnson, K.W.; Phebus, L.A.; Cohen, M.L. Serotonin in migraine: Theories, animal models and emerging therapies. *Prog. Drug Res.* **1998**, *51*, 219–244. [[CrossRef](#)] [[PubMed](#)]

18. Fozard, J.R.; Kalkman, H.O. 5-Hydroxytryptamine (5-HT) and the initiation of migraine: New perspectives. *Naunyn-Schmiedeberg Arch. Pharmacol.* **1994**, *350*, 225–229. [[CrossRef](#)] [[PubMed](#)]
19. Schmuck, K.; Ullmer, C.; Kalkman, H.O.; Probst, A.; Lübbert, H. Activation of Meningeal 5-HT_{2B} Receptors: An Early Step in the Generation of Migraine Headache? *Eur. J. Neurosci.* **1996**, *8*, 959–967. [[CrossRef](#)] [[PubMed](#)]
20. Janssen, W.; Schymura, Y.; Novoyatleva, T.; Kojonazarov, B.; Boehm, M.; Wietelmann, A.; Luitel, H.; Murmann, K.; Krompiec, D.R.; Tretyn, A.; et al. 5-HT_{2B} receptor antagonists inhibit fibrosis and protect from RV heart failure. *Biomed. Res. Int.* **2015**, *2015*, 438403. [[CrossRef](#)] [[PubMed](#)]
21. Zhou, Y.; Ma, J.; Lin, X.; Huang, X.-P.; Wu, K.; Huang, N. Structure-Based Discovery of Novel and Selective 5-Hydroxytryptamine 2B Receptor Antagonists for the Treatment of Irritable Bowel Syndrome. *J. Med. Chem.* **2016**, *59*, 707–720. [[CrossRef](#)] [[PubMed](#)]
22. Bonhaus, D.W.; Flippin, L.A.; Greenhouse, R.J.; Jaime, S.; Rocha, C.; Dawson, M.; Van Natta, K.; Chang, L.K.; Pulido-Rios, T.; Webber, A.; et al. RS-127445: A selective, high affinity, orally bioavailable 5-HT_{2B} receptor antagonist. *Br. J. Pharmacol.* **1999**, *127*, 1075–1082. [[CrossRef](#)] [[PubMed](#)]
23. Thomas, D.R.; Gager, T.L.; Holland, V.; Brown, A.M.; Wood, M.D. m-Chlorophenylpiperazine (mCPP) is an antagonist at the cloned human 5-HT_{2B} receptor. *Neuroreport* **1996**, *7*, 1457–1460. [[CrossRef](#)] [[PubMed](#)]
24. Kovács, A.; Gacsályi, I.; Wellmann, J.; Schmidt, É.; Szűcs, Z.; Dubreuil, V.; Nicolas, J.P.; Boutin, J.; Bózsing, D.; Egyed, A.; et al. Effects of EGIS-7625, a Selective and Competitive 5-HT_{2B} Receptor Antagonist. *Cardiovasc. Drugs Ther.* **2003**, *17*, 427–434. [[CrossRef](#)] [[PubMed](#)]
25. Audia, J.E.; Evrard, D.A.; Murdoch, G.R.; Droste, J.J.; Nissen, J.S.; Schenck, K.W.; Fludzinski, P.; Lucaites, V.L.; Nelson, D.L.; Cohen, M.L. Potent, selective tetrahydro- β -carboline antagonists of the serotonin 2B (5HT_{2B}) contractile receptor in the rat stomach fundus. *J. Med. Chem.* **1996**, *39*, 2773–2780. [[CrossRef](#)] [[PubMed](#)]
26. Forbes, I.T.; Kennett, G.A.; Gadre, A.; Ham, P.; Hayward, C.J.; Martin, R.T.; Thompson, M.; Wood, M.D.; Baxter, G.S. *N*-(1-Methyl-5-indolyl)-*N'*-(3-pyridyl)urea hydrochloride: The first selective 5-HT_{1C} receptor antagonist. *J. Med. Chem.* **1993**, *36*, 1104–1107. [[CrossRef](#)] [[PubMed](#)]
27. Reid, T.-E.; Kumar, K.; Wang, X. Predictive In Silico Studies of Human 5-hydroxytryptamine Receptor Subtype 2B (5-HT_{2B}) and Valvular Heart Disease. *Curr. Top. Med. Chem.* **2013**, *13*, 1353–1362. [[CrossRef](#)] [[PubMed](#)]
28. Lacivita, E.; Podlowska, S.; Speranza, L.; Niso, M.; Satała, G.; Perrone, R.; Perrone-Capano, C.; Bojarski, A.J.; Leopoldo, M. Structural modifications of the serotonin 5-HT₇ receptor agonist *N*-(4-cyanophenylmethyl)-4-(2-biphenyl)-1-piperazinehexanamide (LP-211) to improve in vitro microsomal stability: A case study. *Eur. J. Med. Chem.* **2016**, *120*, 363–379. [[CrossRef](#)] [[PubMed](#)]
29. Rataj, K.; Czarnecki, W.; Podlowska, S.; Bojarski, A.J. Substructural Connectivity Fingerprint and Extreme Entropy Machines—A New Method of Compound Representation and Analysis. *Molecules* **2018**. submitted.
30. Czarnecki, W.M. Weighted Tanimoto Extreme Learning Machine with Case Study in Drug Discovery. *IEEE Comput. Intell. Mag.* **2015**, *10*, 19–29. [[CrossRef](#)]
31. Cortes, C.; Vapnik, V. Support-vector networks. *Mach. Learn.* **1995**, *20*, 273–297. [[CrossRef](#)]
32. Klekota, J.; Roth, F.P. Chemical substructures that enrich for biological activity. *Bioinformatics* **2008**, *24*, 2518–2525. [[CrossRef](#)] [[PubMed](#)]
33. Vass, M.; Ágai-Csongor, É.; Horti, F.; Keserű, G.M. Multiple Fragment Docking and Linking in Primary and Secondary Pockets of Dopamine Receptors. *ACS Med. Chem. Lett.* **2014**, *5*, 1010–1014. [[CrossRef](#)] [[PubMed](#)]
34. Bento, A.P.; Gaulton, A.; Hersey, A.; Bellis, L.J.; Chambers, J.; Davies, M.; Krüger, F.A.; Light, Y.; Mak, L.; McGlinchey, S.; et al. The ChEMBL bioactivity database: An update. *Nucleic Acids Res.* **2014**, *42*, D1083–D1090. [[CrossRef](#)] [[PubMed](#)]
35. Kiss, R.; Sandor, M.; Szalai, F.A. <http://McuLe.com>: A public web service for drug discovery. *J. Cheminform.* **2012**, *4*, P17. [[CrossRef](#)]
36. Ballesteros, J.A.; Weinstein, H. [19] Integrated methods for the construction of three-dimensional models and computational probing of structure-function relations in G protein-coupled receptors. *Methods Neurosci.* **1995**, *25*, 366–428. [[CrossRef](#)]
37. Kristiansen, K.; Kroeze, W.K.; Willins, D.L.; Gelber, E.I.; Savage, J.E.; Glennon, R.A.; Roth, B.L. A highly conserved aspartic acid (Asp-155) anchors the terminal amine moiety of tryptamines and is involved in membrane targeting of the 5-HT_{2A} serotonin receptor but does not participate in activation via a “salt-bridge disruption” mechanism. *J. Pharmacol. Exp. Ther.* **2000**, *293*, 735–746. [[PubMed](#)]

38. Michino, M.; Beuming, T.; Donthamsetti, P.; Newman, A.H.; Javitch, J.A.; Shi, L.; Molinoff, P.B.; Ruffolo, R.R.; Trendelenburg, U. What can crystal structures of aminergic receptors tell us about designing subtype-selective ligands? *Pharmacol. Rev.* **2015**, *67*, 198–213. [[CrossRef](#)] [[PubMed](#)]
39. Kelemen, Á.A.; Kiss, R.; Ferenczy, G.G.; Kovács, L.; Flachner, B.; Lőrincz, Z.; Keserű, G.M. Structure-Based Consensus Scoring Scheme for Selecting Class A Aminergic GPCR Fragments. *J. Chem. Inf. Model.* **2016**, *56*, 412–422. [[CrossRef](#)] [[PubMed](#)]
40. The PubChem Project. Available online: <https://pubchem.ncbi.nlm.nih.gov/> (accessed on 24 January 2018).
41. Moss, N.; Choi, Y.; Cogan, D.; Flegg, A.; Kahrs, A.; Loke, P.; Meyn, O.; Nagaraja, R.; Napier, S.; Parker, A.; et al. A new class of 5-HT_{2B} antagonists possesses favorable potency, selectivity, and rat pharmacokinetic properties. *Bioorgan. Med. Chem. Lett.* **2009**, *19*, 2206–2210. [[CrossRef](#)] [[PubMed](#)]
42. *Schrödinger Release 2017-4: LigPrep*; Schrödinger, LLC: New York, NY, USA, 2017.
43. Berman, H.M. The Protein Data Bank. *Nucleic Acids Res.* **2000**, *28*, 235–242. [[CrossRef](#)] [[PubMed](#)]
44. *Schrödinger Release 2017-4: Schrödinger Suite 2017-4 Protein Preparation Wizard*; Schrödinger, LLC: New York, NY, USA, 2017.
45. *Small-Molecule Drug Discovery Suite 2017-4*; Schrödinger, LLC: New York, NY, USA, 2017.
46. *Schrödinger Release 2017-4: Glide*; Schrödinger, LLC: New York, NY, USA, 2017.
47. Yung-Chi, C.; Prusoff, W.H. Relationship between the inhibition constant (KI) and the concentration of inhibitor which causes 50 per cent inhibition (I50) of an enzymatic reaction. *Biochem. Pharmacol.* **1973**, *22*, 3099–3108. [[CrossRef](#)]

Sample Availability: Samples of the tested compounds are available from commercial vendors.



© 2018 by the authors. Licensee MDPI, Basel, Switzerland. This article is an open access article distributed under the terms and conditions of the Creative Commons Attribution (CC BY) license (<http://creativecommons.org/licenses/by/4.0/>).